JACS
JOURNAL OF THE AMERICAN CHEMICAL SOCIETY
Communication
pubs.acs.org/JACS

Stepwise Synthesis of Robust Metal–Organic Frameworks via Postsynthetic Metathesis and Oxidation of Metal Nodes in a Single-Crystal to Single-Crystal Transformation

Tian-Fu Liu, Lanfang Zou, Dawei Feng, Ying-Pin Chen, Stephen Fordham, Xuan Wang, Yangyang Liu, and Hong-Cai Zhou*

Department of Chemistry, Texas A&M University, College Station, Texas 77842-3012, United States

Supporting Information

ABSTRACT: Utilizing **PCN-426-Mg** as a template, two robust metal-organic frameworks (MOFs), **PCN-426-Fe(III)** and **PCN-426-Cr(III)**, have been synthesized through a strategy of postsynthetic metathesis and oxidation (PSMO) of the metal nodes step by step. The frameworks remained in their single crystal form throughout. Furthermore, the stability and porosity of the frameworks were significantly improved after PSMO. By taking advantage of both the kinetically labile metal–ligand exchange reactions prior to oxidation and the kinetically inert metal–ligand bonds after oxidation, robust MOFs, which would otherwise be difficult to synthesize, can be readily prepared.

Metal–organic frameworks (MOFs) have garnered significant interest in the past two decades due to their promising potential in many applications such as gas adsorption, separation, catalysis, and sensing.[1] Compared with other porous materials such as zeolite and mesoporous silica, MOFs are based on crystalline porous structures tunable on the atomic scale, which is easily designed and functionalized by judicious choice of metal nodes and modification of the organic linkers. However, one of the limitations of most MOFs is their low chemical stability, which undoubtedly hampers their application in industry. A rule of thumb for the construction of stable MOFs comes from the simple Hard and Soft Acid and Base Theory, which guides the selection of the metal–ligand combinations for MOFs.[2] Because the carboxylate group is a hard Lewis base, hard Lewis acids such as Fe^{3+}, Cr^{3+}, Zr^{4+}, and Ti^{4+} are usually considered good candidates for the construction of robust MOFs. This method has become the focus of some recent research efforts, but very few stable MOFs have been obtained, especially in single crystal form.[3] The main reason is that MOFs based on these metal ions of high valence are difficult to crystallize, presumably due to the kinetic inertness of the metal–ligand bonds. Occasionally, MOFs in the form of crystalline powder were obtained, but structure solution and refinement based on powder X-ray diffraction (PXRD) data are not straightforward. Furthermore, the incorporation of rarely reported metal nodes into MOFs is less predictable and controllable. These led us to consider the post-synthetic metathesis and oxidation (PSMO) as an option for the preparation of robust MOFs, by taking advantage of both the kinetically labile metal–ligand exchange reactions prior to oxidation and the kinetically inert metal–ligand bonds after oxidation.

To date, there are about twenty examples of postsynthetic metal metathesis, and most of them occurred between two transition metals categorized as soft or borderline Lewis acids such as Mn(II), Co(II), Ni(II), Cu(II), Zn(II), and Cd(II).[4] However, the success of these metal metatheses did not improve the stability of the MOFs because the resulting metal–ligand bonds were kinetically labile. Cohen and Dincă's groups have initially demonstrated the feasibility of postsynthetic exchange for normally "inert" frameworks or metal ions.[5] However, attaining a complete metal exchange product can be a daunting task due to the inertness of the starting metal–ligand bonds. Moreover, earlier studies indicate that postsynthetic metal metathesis usually requires a long reaction time ranging from a few days to several weeks.[4−6] To overcome the aforementioned difficulties, the following steps are required: (1) select template MOFs with labile metal–ligand bonds; (2) exchange with metal ions that can be oxidized to high oxidation state while preserving the coordination environment around the metal ion.

With these considerations in mind, instead of using the most often encountered transition metal–MOFs, we synthesized a Mg-MOF (denoted as **PCN-426-Mg**, PCN stands for Porous Coordination Network) as a framework template wherein the Mg–O bond is more labile than common coordination bonds. Crystallographic studies revealed that the Mg atoms in **PCN-426-Mg** form the oxo-trinuclear cluster usually observed in both iron and chromium chemistry (Figure 1).[7] This leads to the possibility of applying the PSMO strategy to obtain MOFs of Fe(III) and Cr(III) with the Mg(II)-MOF as a template. To accelerate the exchange process and preserve the overall structure, we first use Fe^{2+} and Cr^{2+}, which have relatively higher exchange rates, to form the intermediate Fe(II)- and Cr(II)-MOFs. After air oxidation, ultra-water-stable MOFs, **PCN-426-Fe(III)** and **PCN-426-Cr(III)**, were obtained in a single-crystal to single-crystal (SC-SC) transformation.[8] Significantly, these MOFs that contain high-valence metals, especially Cr(III), were made almost exclusively in the form of crystalline powders until this work.[9]

Colorless crystals of **PCN-426-Mg** were synthesized by a solvothermal reaction of $Mg(NO_3)_2{\cdot}6H_2O$ and **TMQPTC**

Received: March 6, 2014
Published: May 19, 2014

   dx.doi.org/10.1021/ja5023283 | J. Am. Chem. Soc. 2014, 136, 7813−7816

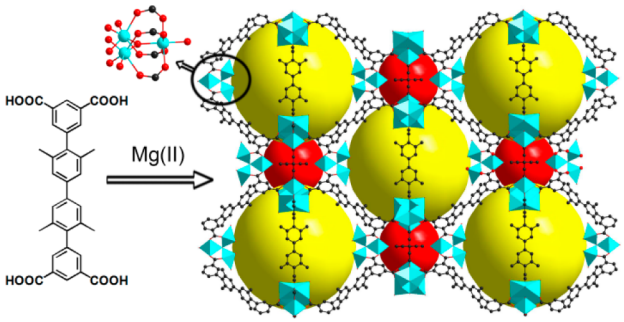

Figure 1. Structure of **PCN-426-Mg**, synthesized from **TMQPTC** ligands and Mg(II) ions.

(2′,3″,5″,6′-tetramethyl-[1,1′:4′,1″:4″,1‴-quaterphenyl] 3,3‴,5,5‴ -tetracarboxylic acid) at 100 °C for 24 h. An X-ray diffraction study reveals that **PCN-426-Mg** crystallizes in the $Fm\bar{3}m$ space group. Each Mg(II) is octahedrally coordinated with three of them sharing a common oxygen to form an $[M_3(\mu_3\text{-O})]$ cluster, which is also common in Cr, Fe, V, Co, Ni, Ru, and Al MOFs.[10]

Further inspection of the structure of **PCN-426-Mg** reveals that each cluster is connected with four carboxylate ligands with the remaining four coordination sites occupied by aqua ligands. This is quite different from previously reported $[M_3(\mu_3\text{-O})]$ clusters, which are usually fully coordinated by carboxylates, giving rise to six connected inorganic nodes. The reduced connectivity of the inorganic nodes and increased number of terminal aqua ligands not only allow easy access for the incoming metal ions during metal-ion exchange but also stabilize the overall framework throughout the metathesis. Furthermore, the $[M_3(\mu_3\text{-O})]$ cluster can accommodate both di- and trivalent metal ions by varying charges on the terminal ligands, the bridging O atom, and/or the counterions. This allows the incorporation of di- and trivalent metal ions in **PCN-426-M** with the original framework structure preserved. Due to its excellent stability, **PCN-426-M(III)** is the desired product. However, one-pot solvothermal reactions between the ligand **TMQPTC** and M(III) salts, such as $FeCl_3$ and $CrCl_3$, failed to yield a crystalline product. For the postsynthetic methods, there are two conceivable routes: the direct metathesis and PSMO. In the following, these two methods will be performed respectively, revealing the drawbacks of direct metathesis and the advantages of PSMO.

After a direct metal metathesis of **PCN-426-Mg** with anhydrous $FeCl_3$ in DMF for 12 h, the crystal changed from colorless to red and became opaque (Figure S6b). However, following a direct metal metathesis of **PCN-426-Mg** with $CrCl_3$ under similar reaction conditions, only a slight color change occurred (Figure S6e). Energy-dispersive X-ray spectroscopy (EDS) studies revealed that 87% of Fe and only a trace amount of Cr were exchanged. This metal exchange procedure includes Mg−O bond dissociation and M−O (M = Fe, Cr) bond formation, which is similar to a simple ligand exchange process in that both are based on the kinetic lability of M−O bonds. Although the exchange rate of a specific metal ion differs from ligand to ligand, the comparison of their water exchange rate can be used to gauge the relative reactivity of two metal ions in postsynthetic exchange. For Fe^{3+}, the ligand exchange reaction rate constant is around 10^2 (k, s^{-1}). For Cr^{3+}, the kinetically inert d^3 configuration results in a much slower reaction rate constant of 10^{-6} (k, s^{-1}).[11] Consequently, even after a long period of time, only part of the Mg^{2+} ions in the inorganic nodes can be exchanged in **PCN-426-Mg** using M^{3+} (Cr^{3+} and Fe^{3+}) ions, although the Fe^{3+} exchange reaction understandably went much further than that of Cr^{3+}.

In addition to the incomplete metal exchange, the PXRD pattern indicates framework decomposition after Mg^{2+}/Fe^{3+} exchange. Since Fe^{3+} and Cr^{3+} are both harder Lewis acidic species than Mg^{2+}, they can competitively bind the carboxylates, which would damage the skeleton of the MOF template. Meanwhile, these hard Lewis acids can undergo hydrolysis during the metal metathesis due to the presence of adventitious water in the template framework. To test this hypothesis, we conducted the previous metal metathesis reactions using $Fe(NO_3)_3{\cdot}6H_2O$ and $Cr(NO_3)_3{\cdot}6H_2O$ instead of anhydrous $FeCl_3$ and $CrCl_3$ to intentionally introduce water molecules. With $Fe(NO_3)_3{\cdot}6H_2O$, the color of the crystal changed to red followed by decomposition of the framework and the appearance of a white precipitate in 12 h (Figure S6c). For $Cr(NO_3)_3{\cdot}6H_2O$, the **PCN-426-Mg** crystal completely decomposed to form a homogeneous solution (Figure S6f). The hydrolysis equilibrium constant of Fe^{3+} and Cr^{3+} (pK_a = 2.2 and 4 respectively) is much larger than that of Fe^{2+} and Cr^{2+} (pK_a = 9.5 and 10 respectively) creating a higher aqueous proton concentration in the metal metathesis reaction.[12] An acidic environment is detrimental to the fragile Mg−O bond and induces the decomposition of the framework. Moreover, the loss of crystallinity can greatly impair the diffusion of metal ions, which hampers further metal exchange, leading to incomplete metathesis. This control experiment has exposed the disadvantage of direct metal metathesis with M^{3+} species: (1) Fe^{3+} and Cr^{3+} have very low ligand exchange rates and display kinetic inertness; and (2) larger hydrolysis equilibrium constants produce more acidic environments destroying the integrity of the MOFs.

In conclusion, the direct metal metathesis of Mg^{2+}/Fe^{3+} or Mg^{2+}/Cr^{3+} is not a viable synthetic route toward stable high-valence MOFs. In view of the much higher ligand exchange rate and smaller hydrolysis equilibrium constant of Fe^{2+} and Cr^{2+}, herein a PSMO strategy is proposed, which represents a stepwise synthesis of MOFs via postsynthetic metathesis with low-valence metal ions and followed by the oxidation of metal nodes. First, the as-synthesized **PCN-426-Mg** crystals were washed with dry DMF several times and bubbled with nitrogen for 15 min, and anhydrous $FeCl_2$ was added under the protection of nitrogen. This resulted in an evident color change of the crystals from colorless to purple in merely 20 min with complete exchange after 3 h. In general, the concentration difference is the major driving force for metal exchange, which can also be described as the entropic force. On the other hand, the degree of metal exchange is most likely controlled by the stability constant of the metal ions. As Fe(II) and Cr(II) complexes have higher stabilities than that of the Mg(II) complex, Fe^{2+} and Cr^{2+} ions have an increased tendency toward complex formation.[13] The above-mentioned two aspects contribute to the success of metal exchange between Mg(II) and Fe(II)/Cr(II). After metal exchange, the excess $FeCl_2$ solution was removed with a syringe, and the solid was washed with fresh DMF to yield light brown crystals as shown in Figure 2b. The sample was suspended in an aliquot of DMF and bubbled with an air stream for 15 min, causing an apparent color change of the crystal to dark brown as shown in Figure 2c. Single crystal X-ray diffraction (Table S1), X-ray photoelectron spectroscopy (Figures S7 and S8), and an EDS spectrum (Figure 3g, Figure S13) have confirmed that the PSMO procedure was accomplished in an SC-SC transformation to give

dx.doi.org/10.1021/ja5023283 | J. Am. Chem. Soc. 2014, 136, 7813−7816

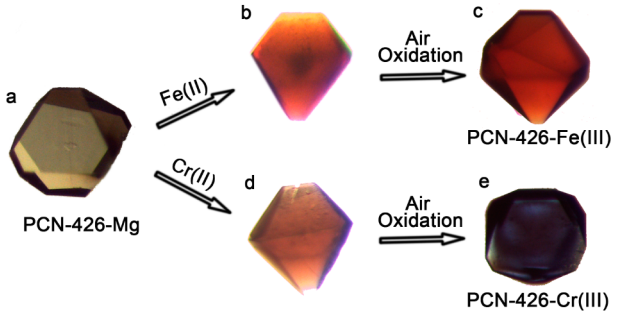

Figure 2. Optical microscope photographs of (a) as-synthesized **PCN-426-Mg**, (b) **PCN-426-Mg** after metathesis with $FeCl_2$ for 3 h, (c) **PCN-426-Fe**(III) after metal node oxidation, (d) **PCN-426-Mg** after metathesis with $CrCl_2$ for 3 h, and (e) **PCN-426-Cr(III)** after metal node oxidation.

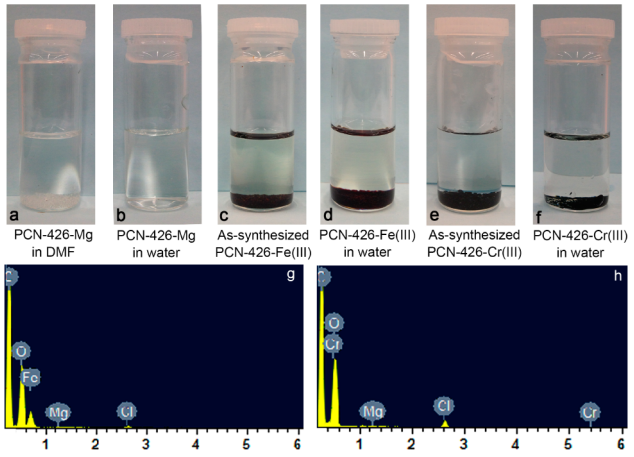

Figure 3. View of the (a) as-synthesized **PCN-426-Mg**, (b) **PCN-426-Mg** dissolved in water, (c) as-synthesized **PCN-426-Fe(III)**, (d) **PCN-426-Fe(III)** immersed in water, (e) as-synthesized **PCN-426-Cr(III)**, (f) **PCN-426-Cr(III)** immersed in water, (g) the EDS spectrum of **PCN-426-Fe(III)**, and (h) **PCN-426-Cr(III)**.

PCN-426-Fe(III). **PCN-426-Cr(III)** was synthesized through the same PSMO method using anhydrous $CrCl_2$, yielding an even more evident color change from colorless to brown after metathesis and finally to dark blue upon oxidation (Figure 2d and 2e). Single crystal X-ray crystallographic studies indicate that these new MOFs are isostructural with the Mg-MOF template, which is otherwise unachievable through the direct reaction of the **TMQPTC** ligand and Fe^{3+}/Fe^{2+} or Cr^{3+}/Cr^{2+} metal source. The successful synthesis of **PCN-426-Fe(III)** and **PCN-426-Cr(III)** illustrate the overwhelming advantages of PSMO: (1) the stepwise strategy makes the metal metathesis much faster and more complete. The primary advantage is on account of the substantial improvement in ligand exchange rates, which is an up to 10^5-fold increase from Fe^{3+} (10^2 (k, s^{-1})) to Fe^{2+} (10^7 (k, s^{-1})) and an as large as 10^{16}-fold improvement from Cr^{3+} (10^{-6} (k, s^{-1})) to Cr^{2+} (10^{10} (k, s^{-1})) due to the electron configuration changes from d^3 to d^4. PSMO also alleviates the challenges of partial exchange and kinetic inertness. (2) Fe^{2+} and Cr^{2+} are softer Lewis acids, which interact more weakly with the carboxylate ligand (a hard Lewis base) than hard Lewis acids such as Fe^{3+} and Cr^{3+}, so the metal metathesis can be conducted with less destruction of crystallinity. (3) Metal ions with smaller hydrolysis equilibrium constants provide relatively milder conditions where the framework template remains intact during the exchange and facilitates the transportation of metal ions toward metal exchange completion. (4) The subsequent air oxidation is a very gentle but effective postsynthetic treatment.

After the labile Mg−O bonds have been replaced by inert Fe(III)−O and Cr(III)−O bonds, the stability of the frameworks was greatly improved. As shown in Figure 3, **PCN-426-Mg** was dissolved immediately after immersion in water, while **PCN-426-Fe(III)** is stable in water after 1 day. PXRD patterns confirm that the framework is stable in aqueous solutions with pH values 4–10 (Figure 4). Although Cr(III), compared to Fe(III), has the same valence and a similar radius, its kinetic inertness has resulted in the remarkable stability of **PCN-426-Cr(III)**, which is much higher than that of **PCN-426-Fe(III)**. PXRD studies indicated that the crystallinity of **PCN-426-Cr(III)** remains intact from pH = 12 to extremely acidic conditions (4 M HCl) for at least 12 h (Figure 4). Benefiting from the improved stability, both **PCN-426-Fe(III)** and **PCN-426-Cr(III)** exhibit permanent porosity whereas **PCN-426-Mg** does not, as shown by N_2 adsorption isotherms (Figure 5). Brunauer–Emmett–Teller (BET) surface areas of 2132 and 3155 m^2/g (Langmuir surface area of 2623 and 3883 m^2/g) were observed for **PCN-426-Fe(III)** and **PCN-426-Cr(III)**, respectively. Compared with **PCN-426-Fe(III)**, the higher N_2 uptake of **PCN-426-Cr(III)** can probably be ascribed to the higher exchange rate of the Cr^{2+}

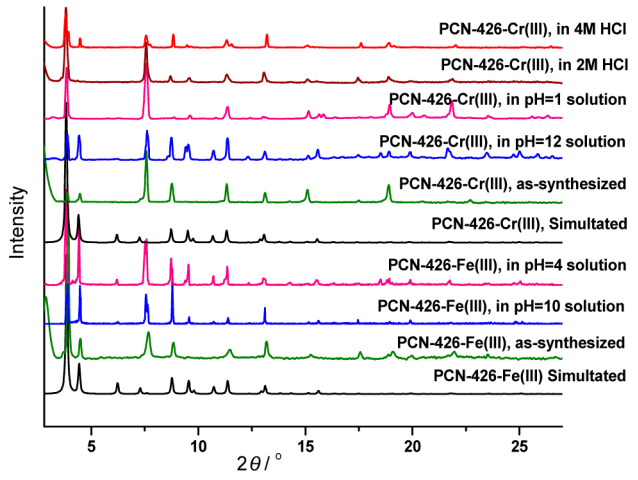

Figure 4. PXRD patterns of as-synthesized **PCN-426-Fe(III)**, and **PCN-426-Cr(III)** as well as samples treated with a variety of aqueous solutions.

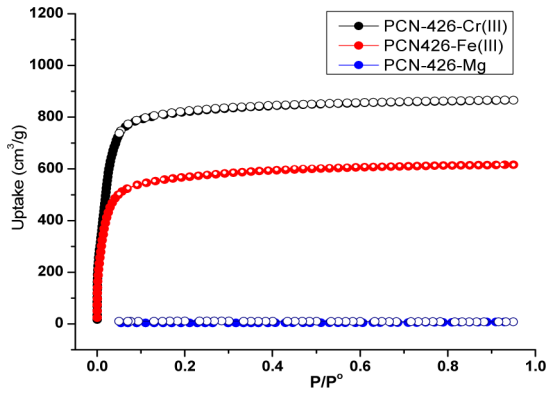

Figure 5. N_2 adsorption isotherms of **PCN-426-Mg**, **PCN-426-Fe(III)**, and **PCN-426-Cr(III)**.

dx.doi.org/10.1021/ja5023283 | J. Am. Chem. Soc. 2014, 136, 7813–7816

ion, which makes the metal exchange process complete within a short period of time thus minimizes the loss of crystallinity. Moreover, the higher stability of **PCN-426-Cr(III)**, as revealed in Figure 4, also contributes to a higher N_2 uptake. The least stable framework **PCN-426-Mg** collapsed after activation and failed to exhibit permanent porosity.

In summary, robust Fe(III) and Cr(III) MOFs with improved water stability and porosity can be synthesized using a PSMO strategy step by step. This strategy can overcome the challenges of incomplete exchange and low exchange rate, which are commonly encountered in the preparation of high-valence MOFs by metathesis. Here, the following has been demonstrated: (1) A Mg-MOF was chosen as a template so that the labile M−O bonds can drive the metal exchange to completion; (2) the MOF template was first exchanged with low-oxidation-state but kinetically labile metal ions, which were subsequently oxidized to a high oxidation state to accelerate the metal exchange and at the same time preserve the integrity of the framework. The completely exchanged products **PCN-426-Fe(III)** and **PCN-426-Cr(III)** were obtained in an SC-SC transformation procedure and characterized by single crystal X-ray diffraction studies. In general, chromium MOFs were obtained in powder forms almost exclusively in the literature until **PCN-426-Cr(III)**, which have been made through the PSMO synthetic route. Because MOFs based on high-valence metal ions are usually produced in amorphous or powder forms, PSMO is of critical importance for the synthesis and characterization of robust MOFs, which are otherwise difficult or unfeasible through traditional synthetic routes.

■ ASSOCIATED CONTENT

Ⓢ Supporting Information

Full details for sample preparation, characterization, and crystallographic studies (CIF). This material is available free of charge via the Internet at http://pubs.acs.org.

■ AUTHOR INFORMATION

Corresponding Author

zhou@mail.chem.tamu.edu

Notes

The authors declare no competing financial interest.

■ ACKNOWLEDGMENTS

This work was supported as part of the Center for Gas Separations Relevant to Clean Energy Technologies, an Energy Frontier Research Center funded by the U.S. Department of Energy (DOE), Office of Science, Office of Basic Energy Sciences under Award Number DE-SC0001015.

■ REFERENCES

(1) (a) Yaghi, O. M.; O'Keeffe, M.; Ockwig, N. W.; Chae, H. K.; Eddaoudi, M.; Kim, J. *Nature* **2003**, *423*, 705. (b) Ferey, G.; Mellot-Draznieks, C.; Serre, C.; Millange, F. *Acc. Chem. Res.* **2005**, *38*, 217. (c) Horike, S.; Shimomura, S.; Kitagawa, S. *Nat. Chem.* **2009**, *1*, 695. (d) Seo, J. S.; Whang, D.; Lee, H.; Jun, S. I.; Oh, J.; Jeon, Y. J.; Kim, K. *Nature* **2000**, *404*, 982. (e) Jiang, H.-L.; Liu, B.; Akita, T.; Haruta, M.; Sakurai, H.; Xu, Q. *J. Am. Chem. Soc.* **2009**, *131*, 11302. (f) Kreno, L. E.; Leong, K.; Farha, O. K.; Allendorf, M.; Van Duyne, R. P.; Hupp, J. T. *Chem. Rev.* **2012**, *112*, 1105. (g) Yang, S.; Liu, L.; Sun, J.; Thomas, K. M.; Davies, A. J.; George, M. W.; Blake, A. J.; Hill, A. H.; Fitch, A. N.; Tang, C. C.; Schröder, M. *J. Am. Chem. Soc.* **2013**, *135*, 4954. (h) Bloch, E. D.; Queen, W. L.; Krishna, R.; Zadrozny, J. M.; Brown, C. M.; Long, J. R. *Science* **2012**, *335*, 1606. (i) Wang, Z.; Cohen, S. M. *Chem. Soc. Rev.* **2009**, *38*, 1315.

(2) Pearson, R. G. *J. Am. Chem. Soc.* **1963**, *85*, 3533.

(3) (a) Cavka, J. H.; Jakobsen, S.; Olsbye, U.; Guillou, N.; Lamberti, C.; Bordiga, S.; Lillerud, K. P. *J. Am. Chem. Soc.* **2008**, *130*, 13850. (b) Ferey, G.; Serre, C. *Chem. Soc. Rev.* **2009**, *38*, 1380. (c) Phan, A.; Doonan, C. J.; Uribe-Romo, F. J.; Knobler, C. B.; O ' Keeffe, M.; Yaghi, O. M. *Acc. Chem. Res.* **2010**, *43*, 58. (d) Murray, L. J.; Dincă, M.; Yano, J.; Chavan, S.; Bordiga, S.; Brown, C. M.; Long, J. R. *J. Am. Chem. Soc.* **2010**, *132*, 7856. (e) Feng, D.; Gu, Z.-Y.; Li, J.-R.; Jiang, H.-L.; Wei, Z.; Zhou, H.-C. *Angew. Chem., Int. Ed.* **2012**, *51*, 10307. (f) Jiang, H.-L.; Feng, D.; Liu, T.-F.; Li, J.-R.; Zhou, H.-C. *J. Am. Chem. Soc.* **2012**, *134*, 14690.

(4) (a) Lalonde, M.; Bury, W.; Karagiaridi, O.; Brown, Z.; Hupp, J. T.; Farha, O. K. *J. Mater. Chem. A* **2013**, *1*, 5453. (b) Brozek, C. K.; Cozzolino, A. F.; Teat, S. J.; Chen, Y.-S.; Dincă, M. *Chem. Mater.* **2013**, *25*, 2998.

(5) (a) Kim, M.; Cahill, J. F.; Fei, H.; Prather, K. A.; Cohen, S. M. *J. Am. Chem. Soc.* **2012**, *134*, 18082. (b) Brozek, C. K.; Dincă, M. *J. Am. Chem. Soc.* **2013**, *135*, 12886.

(6) (1) Dincă, M.; Long, J. R. *J. Am. Chem. Soc.* **2007**, *129*, 11172. (2) Kim, Y.; Das, S.; Bhattacharya, S.; Hong, S.; Kim, M. G.; Yoon, M.; Natarajan, S.; Kim, K. *Chem.—Eur. J.* **2012**, *18*, 16642.

(7) (a) Serre, C.; Mellot-Draznieks, C.; Surblé, S.; Audebrand, N.; Filinchuk, Y.; Férey, G. *Science* **2007**, *315*, 1828. (b) Tranchemontagne, D. J.; Mendoza-Cortes, J. L.; O'Keeffe, M.; Yaghi, O. M. *Chem. Soc. Rev.* **2009**, *38*, 1257.

(8) (a) Halder, G. J.; Kepert, C. J. *Aust. J. Chem.* **2006**, *59*, 597. (b) MacGillivray, L. R.; Papaefstathiou, G. S.; Friščićs, T.; Hamilton, T. D.; Bučar, D.-K.; Chu, Q.; Varshney, D. B.; Georgiev, I. G. *Acc. Chem. Res.* **2008**, *41*, 280.

(9) (a) Férey, G.; Mellot-Draznieks, C.; Serre, C.; Millange, F.; Dutour, J.; SurbléS; Margiolaki, I. *Science* **2005**, *309*, 2040. (b) Férey, G.; Serre, C.; Mellot-Draznieks, C.; Millange, F.; Surblé, S.; Dutour, J.; Margiolaki, I. *Angew. Chem., Int. Ed.* **2004**, *43*, 6296. (c) Serre, C.; Millange, F.; Thouvenot, C.; Noguës, M.; Marsolier, G.; Louër, D.; Férey, G. *J. Am. Chem. Soc.* **2002**, *124*, 13519.

(10) (a) Seo, S.; Whang, D.; Lee, H.; Jun, S.; Oh, J.; Jeon, Y.; Kim, K. *Nature* **2000**, *404*, 982. (b) Sudik, A. C.; Millward, A. R.; Ockwig, N. W.; Côté, A. P.; Kim, J.; Yaghi, O. M. *J. Am. Chem. Soc.* **2005**, *127*, 7110. (c) Férey, G.; Mellot-Draznieks, C.; Serre, C.; Millange, F.; Dutour, J.; Surblé, S.; Margiolaki, I. *Science* **2005**, *309*, 2040. (d) Sudik, A. C.; Côté, A. P.; Wong-Foy, A. G.; O'Keeffe, M.; Yaghi, O. M. *Angew. Chem., Int. Ed.* **2006**, *45*, 2528. (e) Zhang, Y.-B.; Zhang, W.-X.; Feng, F.-Y.; Zhang, J.-P.; Chen, X.-M. *Angew. Chem., Int. Ed.* **2009**, *48*, 5287. (f) Zheng, S.-T.; Bu, J. T.; Li, Y.; Wu, T.; Zuo, F.; Feng, P.; Bu, X. *J. Am. Chem. Soc.* **2010**, *132*, 17062. (g) Bohnsack, A. M.; Ibarra, I. A.; Hatfield, P. W.; Yoon, J. W.; Hwang, Y. K.; Chang, J.-S.; Humphrey, S. M. *Chem. Commun.* **2011**, *47*, 4899. (h) Jiang, G.; Wu, T.; Zheng, S.-T.; Zhao, X.; Lin, Q.; Bu, X.; Feng, P. *Cryst. Growth Des.* **2011**, *11*, 3713. (i) Zheng, S.-T.; Bu, J. J.; Wu, T.; Chou, C.; Feng, P.; Bu, X. *Angew. Chem., Int. Ed.* **2011**, *50*, 8858. (j) Barthelet, K.; Riou, D.; Férey, G. *Chem. Commun.* **2002**, 1492. (k) Ma, S. Q.; Yuan, D.; Chang, J.-S.; Zhou, H.-C. *Inorg. Chem.* **2009**, *48*, 5398.

(11) Eigen, M. *Pure Appl. Chem.* **1963**, *6*, 105.

(12) (a) Baes, C. F.; Mesmer, R. E.; *The Hydrolysis of Cations*; Wiley-Interscience: New York, 1976. (b) Burgess, J. *Metal Ions in Solutions*; Ellis Horwood: Chichester, U.K., 1978; p 264.

(13) Irving, H.; Williams, R. J. P. *J. Chem. Soc.* **1953**, 3192.